Properties of *p*-Cresol Methylhydroxylase Flavoprotein Overproduced by *Escherichia coli*†

Stefan Engst,‡ Vladislav Kuusk,§ Igor Efimov, Ciarán N. Cronin, and William S. McIntire*

Molecular Biology Division, Department of Veterans Affairs Medical Center, San Francisco, California 94121, and Department of Biochemistry and Biophysics, University of California, San Francisco, California 94143

Received June 3, 1999; Revised Manuscript Received October 8, 1999

ABSTRACT: The $\alpha_2\beta_2$ flavocytochrome *p*-cresol methylhydroxylase (PCMH) from *Pseudomonas putida* is composed of a flavoprotein homodimer (α_2 or $PchF_2$; $M_r = 119$ kDa) with a cytochrome monomer (β, PchC; $M_r = 9.3$ kDa) bound to each PchF subunit. *Escherichia coli* BL21(DE3) has been transformed with a vector for expression of the *pchF* gene, and PchF is overproduced by this strain as the homodimer. During purification, it was recognized that some PchF had FAD bound, while the remainder was FAD-free. However, unlike PchF obtained from PCMH purified from *P. putida*, FAD was bound noncovalently. The FAD was conveniently removed from purified *E. coli*-expressed PchF by hydroxyapatite chromatography. Fluorescence quenching titration indicated that the affinity of apo-PchF for FAD was sufficiently high to prevent the determination of the dissociation constant. It was found that *p*-cresol was virtually incapable of reducing PchF with noncovalently bound FAD ($PchF^{NC}$), whereas 4-hydroxybenzyl alcohol, the intermediate product of *p*-cresol oxidation by PCMH, reduced $PchF^{NC}$ fairly quickly. In contrast, *p*-cresol rapidly reduced PchF with covalently bound FAD ($PchF^{C}$), but, unlike intact PCMH, which consumed 4 electron equiv/mol when titrated with *p*-cresol (2 electrons from *p*-cresol and 2 from 4-hydroxybenzyl alcohol), $PchF^{C}$ accepted only 2 electron equiv/mol. This is explained by extremely slow release of 4-hydroxybenzyl alcohol from reduced $PchF^{C}$. 4-Hydroxybenzyl alcohol rapidly reduced $PchF^{C}$, producing 4-hydroxybenzaldehyde. It was demonstrated that *p*-cresol has a charge-transfer interaction with FAD when bound to oxidized $PchF^{NC}$, whereas 4-bromophenol (a substrate analogue) and 4-hydroxybenzaldehyde have charge-transfer interactions with FAD when bound to either $PchF^{C}$ or $PchF^{NC}$. This is the first example of a "wild-type" flavoprotein, which normally has covalently bound flavin, to bind flavin noncovalently in a stable, redox-active manner.

p-Cresol methylhydroxylase (PCMH;[1] EC 1.17.99.1), an $\alpha_2\beta_2$ flavocytochrome, has FAD linked via the 8α-carbon of the flavin to the phenolate oxygen of Tyr-384 in each α flavoprotein (PchF) (*1, 2*). Approximately 10% of all known flavoproteins have FMN or FAD covalently tethered to the polypeptide (*3*). Until recently, there was no apparent relationship among covalent flavoproteins that catalyze substantially different reactions. Now it is known that PCMH is a member of a superclass of proteins, some of which bind FAD covalently, while others bind FAD noncovalently (*4*).

Current evidence indicates that tethering of FAD or FMN to respective apo-proteins does not require external agents (e.g., enzymes) (*3*). This is not strictly true for PCMH. We have demonstrated that FAD will not become covalently bound to PchF unless the cytochrome subunit (PchC) is present (*1*). It was also shown that nucleophilic attack by the Tyr-384 phenolate oxygen at the 8α-carbon of the iminoquinone methide form of FAD resulted in two-electron reduced covalently bound FAD. This confirmed a long-standing hypothetical mechanism for self-catalytic attachment of flavin to amino acyl side groups, and PCMH is the first and only case where this chemical mechanism has been definitively substantiated (*1*). The two-electron reduced flavin is reoxidized by electron transfers to the heme of PchC, the same route used during catalytic *p*-cresol oxidation by bound FAD (*5*). For a more extensive discussion of covalent flavoproteins, see reference *3*.

Previously, we reported the expression of *pchF* and *pchC* in *Escherichia coli* DH5α (*6*). When *E. coli*-produced PchF was purified in the absence of PchC, the PchF homodimer was devoid of FAD, and we did not observe FAD binding to apo-PchF, although apo-PchF could be converted quantitatively into PCMH when exposed to stoichiometric amounts of FAD and PchC. After short storage at −70 °C, most of the apo-PchF lost the ability to form PCMH under

† This research was supported by a Department of Veterans Affairs Merit Review Grant, a Program Project Grant (HL-16251) from the National Heart, Lung and Blood Institute of the National Institutes of Health, an Academic Senate Grant, and a Research Evaluation and Allocation Committee Grant, University of California, San Francisco.

* To whom correspondence should be addressed at the Molecular Biology Division (151-S), Department of Veterans Affairs Medical Center, 4150 Clement St., San Francisco, CA 94121. Telephone: 415-387-1431; Fax: 415-750-6959; Email: wsm@itsa.ucsf.edu.

‡ Current address: Exelixis Pharmaceuticals, Inc., 280 E. Grand Ave., South San Francisco, CA 94080.

§ Current address: OREAD, Inc., 3401P Hillview Ave., Palo Alto, CA 94304.

[1] Abbreviations: PchC and PchF, unassociated cytochrome and flavoprotein subunit, respectively, of *p*-cresol methylhydroxylase; *pchC* and *pchF*, genes for the subunits; $PchF^{C}$ and $PchF^{NC}$, PchF with covalently bound and noncovalently bound FAD, respectively; PCMH, *p*-cresol methylhydroxylase; PCR, polymerase chain reaction; SDS, sodium dodecyl sulfate; VAO, vanillyl alcohol oxidase.

10.1021/bi991273d CCC: $18.00
Published on Web 11/24/1999

the same conditions, and the PchF sample required repurification for further use. We believe that the preparative isoelectric focusing used to prepare pure apo-PchF (*1*) is deleterious to the protein.

Herein, we report the properties of pure apo-PchF produced from a newly engineered construct in *E. coli* BL21-(DE3). We have developed a new purification procedure for apo-PchF, which avoids the use of preparative isoelectric focusing. With respect to its ability to be converted into PCMH, it behaved like the apo-PchF studied earlier, but unlike the previously studied form, the new apo-PchF is stable. It was shown that the current form of PchF binds FAD tightly, but noncovalently. The properties of PchF containing covalently bound and noncovalently bound FAD are reported below.

MATERIALS AND METHODS

Materials. Synthetic oligonucleotides were purchased from Operon. Recombinant proteins were produced in *E. coli* BL21(DE3) (Novagen). All other molecular biology experiments reported in this paper utilized *E. coli* DH5αF′IQ (Life Technologies) as host. Sodium dithionite was from Kodak Chemical Co., and disodium 2,6-dichlorophenolindophenol was from General Biochemicals, Inc. Glucose oxidase was purchased from Miles Laboratories. The Mono Q HR10/10, Mono P HR 5/20, and HiLoad 26/10 Q-Sepharose Fast Flow columns and Polybuffer 74 were obtained from Amersham Pharmacia Biotech. Macro-Prep Ceramic Hydroxyapatite, type I, was from Bio-Rad. *p*-Cresol (4-methylphenol) was Aldrich Gold Label grade. The reagents for enzyme purification and other research were purchased from Sigma Chemical Co. or Aldrich Chemical Co. 4-Hydroxybenzyl alcohol was purified by reverse-phase chromatography using a 1 × 30 cm column packed with octadecyl-silica gel (40 μm, average particle diameter; bulk packing for flash chromatography from J. T. Baker, Inc.). The eluting solvent was 3:7 methanol/water (v/v). The solvent was removed by rotary evaporation under vacuum, followed by lyophilization. 4-Hydroxybenzaldehyde was purified by twice subliming, and 4-bromophenol by recrystallization from ethanol/ether. PchC and PchF with covalently bound FAD ($PchF^{C}$) were separated from PCMH as described elsewhere (*6*).

Construction of Expression Vectors for the Production of Recombinant PchC, PchF, and PCMH in E. coli. A restriction site for *Nde*I encompassing the translational start codon of the *pchC* gene was introduced by using the polymerase chain reaction (PCR) with plasmid pUC-9869SmaA as template and the oligonucleotides oPchC5 (5′-GAG.CAA-.CAT.ATG.ACA.TTT.CCC.TTT.AGC.GGC-3′) and oPchC3 (5′-ATA.CGG.ATC.CAA.GCT.TCC.TCA.AGG.CTG.AG-C.CGC.TGG-3′) as amplification primers (underlined bases are those differing from the target template). pUC-9869SmaA consists of the 2.9 kb *Sma*I fragment from *Pseudomonas putida* 9869 plasmid pRA500 (*6*) cloned into the *Sma*I site of pUC18, with the *pchC* gene toward the *Hin*dIII site of the polylinker (also see reference *7*). The PCR-amplified fragment was digested with *Nde*I/*Bam*HI (sites present in the primers only) and cloned between the *Nde*I/*Bam*HI sites of the *E. coli* protein expression vector pET11a (Novagen) to generate plasmid pET-PchC. The integrity of the PCR process was assessed by DNA sequencing of the amplified fragment using T7 promoter and terminator primers (Novagen).

To construct an expression vector for the production of both PchC and PchF, the *pchC* gene from pET-PchC was transferred as a *Xba*I/*Bam*HI fragment to the same sites in pBluescript KS+ (Stratagene) to yield pKS-PchC. A 2.6 kb *Bsm*FI/*Bam*HI fragment from pUC-9869SmaB (similar to pUC-9869SmaA described above but with the cloned insert in the opposite orientation) containing part of *pchC* and the complete structural genes encoding the PchX and PchF proteins (*7*) was cloned between the *Bsm*FI/*Bam*HI sites of pKS-PchC to generate pKS-PCMH. The *Nde*I/*Bam*HI fragment from pKS-PCMH was then transferred between the same sites in pET11a to produce the PCMH expression vector pET-PCMH.

An expression vector for the production of PchF alone was constructed by first introducing a restriction site for *Nde*I encompassing the translational start codon of *pchF* by PCR, using plasmid pKS-PCMH as template and the oligonucleotides oPchF5 (5′-AGG.ATC.TAG.ACA.TAT.GTC.CGA.G-CA.AAA.CAA.TGC.TGT.GTT.GC-3′) and oPchF3 (5′-ACC.GAA.CTC.GAG.CCC.AGT.GGA.GAT.GGT.CCA.GAT.CGG-3′) as amplification primers. The amplified 295 bp fragment encoding the 5′ end of *pchF* was digested with *Xba*I/*Xho*I (sites present in the primers only) and cloned between the *Xba*I/*Xho*I sites of pBluescript II KS+ (Stratagene) to generate pKSII-PchFf. The integrity of the PCR process was assessed by DNA sequencing of the amplified fragment using T7 and T3 promoter primers. The 226 bp *Nde*I/*Bgl*II fragment from pKSII-PchFf was then used to replace the 1275 bp *Nde*I/*Bgl*II fragment in pKS-PCMH to yield pKS-PchF. The *Nde*I/*Bam*HI fragment from pKS-PchF was then transferred between the same sites in pET11a to produce the *pchF* expression vector pET-PchF. *E. coli* BL21-(DE3) transformed with pET-PchC, pET-PCMH, or pET-PchF was used for the production of the respective recombinant proteins. DNA sequence determinations and computer analyses of DNA sequence data were carried out as described previously (*8*).

Purification of $PchF^{NC}$ (PchF with Noncovalently Bound FAD). *E. coli* BL21(DE3) transformed with pET-PchF was grown at 30 °C in Luria−Bertani medium, until an OD_{600} of 0.8−0.9 was attained, and then isopropyl-1-thio-β-D-galactopyranoside was added to a final concentration of 40 μM, and cell growth continued overnight. The typical yield was 25 g of cell paste from 6 L of medium.

PchF was released from the *E. coli* periplasm by using the antibiotic Polymyxin B, in the presence of EDTA. This treatment renders the cell wall permeable to large molecules (*9*, *10*). After harvesting the cells by centrifugation at 6500*g* for 15 min, 25 g of cell paste was resuspended in 100 mL of 10 mM Tris-HCl, 150 mM NaCl, and 5 mM EDTA, pH 7.9 (pH adjusted at 21 °C) (buffer A), and the suspension centrifuged at 6500*g* for 15 min. The cells were resuspended in 50 mL of buffer A (2 mL of buffer per 1 g of cell paste), which also contained 1 mg/mL Polymyxin B. The suspension was stirred slowly for 1 h, and then centrifuged at 17400*g* for 15 min. This procedure was repeated with the resuspended pellet. FAD was added in a 1.5-fold molar excess to the combined supernatants (assuming that 30 mg of PchF subunits were present), and the extract was dialyzed in the dark for 4−5 h against 10 mM Tris-HCl, pH 7.9 (buffer B). Afterward, the sample was centrifuged at 337000*g* for 1 h. The resulting supernatant was applied to a HiLoad 26/10

Q-Sepharose Fast Flow column that had been previously equilibrated in buffer B. The column was washed with 5 volumes of buffer B at 10 mL/min, followed by a 1 h gradient from 0 to 300 mM NaCl in buffer B to separate proteins. $PchF^{NC}$ fractions were combined cautiously to minimize contamination by an *E. coli* cytochrome, which eluted prior to $PchF^{NC}$. Free FAD also eluted from the column before the $PchF^{NC}$ peak. The $PchF^{NC}$ fraction was initially concentrated by using an Amicon pressure concentrator fitted with a YM-30 membrane, and then further concentrated by using Amicon Centricon-30 centrifuge concentrators. The $PchF^{NC}$ sample was loaded onto a Macro-Prep Ceramic Hydroxyapatite column (1 × 10 cm) equilibrated with 10 mM potassium phosphate buffer, pH 7.5. Proteins were eluted with a 10−500 mM potassium phosphate gradient in 1 h, at 2 mL/min. PchF fractions, now devoid of FAD and contaminating cytochrome (as assessed by UV−visible spectroscopy), were collected.

The final step in the purification involved chromatofocusing on a Mono P HR 5/20 column. After equilibrating the column with 25 mM 1,3-bis[tris(hydroxymethyl)methylamino]propane hydrochloride buffer, pH 6.4, the protein was applied with a flow rate of 1 mL/min. The column was washed with this buffer for 1 min, and then the pH gradient was generated by switching to a 6% (v/v) solution of Polybuffer 74, which had been adjusted to pH 3.95 with HCl. Apo-PchF eluted at 19.1 min (pH ∼5.0). Immediately after elution, the pH of the apo-PchF sample was brought to ∼7 by the addition of a small volume of 1 M potassium phosphate buffer, pH 7.2. The components of the Polybuffer were removed by several rounds of centrifugation−concentration (Centricon-30), using 100 mM potassium phosphate buffer, pH 7.2. The typical yield of purified apo-PchF was 25−30 mg from 25 g of cell paste.

Steady-State Kinetic Assays. Phenazine ethosulfate/2,6-dichlorophenolindophenol assays were carried out as described earlier (*5*). Horse heart cytochrome *c* was used also as an electron acceptor in steady-state kinetic assays of PCMH, $PchF^{C}$, and $PchF^{NC}$ (*5*).

Spectroscopy and Titrations. All UV−visible spectral work was carried out with Hewlett-Packard 8451A or 8453A diode array spectrophotometers at 25 °C. Anaerobic reductive $Na_2S_2O_4$ (dithionite) titrations of proteins were carried out in anaerobic quartz cuvettes, as described elsewhere (*11*). Anaerobic dithionite solutions were standardized by titrating anaerobic solutions of FAD ($\epsilon_{445} = 11.3\ mM^{-1}\ cm^{-1}$). For anaerobic *p*-cresol and 4-hydroxybenzyl alcohol reductive titrations, oxygen was scavenged from solutions by the presence of 50 mM glucose, 50 μg/mL glucose oxidase, and 3−6 μg/mL catalase. The concentrations of *p*-cresol and 4-hydroxybenzyl alcohol were determined by using $\epsilon_{276} = 1.71\ mM^{-1}\ cm^{-1}$ (*12*). A published $\epsilon_{442} = 11.7\ mM^{-1}\ cm^{-1}$ was used to determine the concentration of $PchF^{C}$ (*12*). Extinction coefficients were estimated also for $PchF^{C}$ and $PchF^{NC}$ by taking spectra before and after denaturation with 1.8−2.0% (w/v) SDS. It was assumed that the extinction coefficients of the 445 nm peak for the two denatured proteins were identical to that of free FAD. For $PchF^{NC}$, ϵ_{440} was estimated to be $12.6\ mM^{-1}\ cm^{-1}$, and for $PchF^{C}$, ϵ_{443} was estimated to be $12.7\ mM^{-1}\ cm^{-1}$.

$PchF^{C}$ and $PchF^{NC}$ were aerobically titrated with *p*-cresol, the substrate analogue 4-bromophenol, and 4-hydroxybenzaldehyde. Dissociation constants were determined from the spectral titration data using the Factor Analysis Program SPECFIT (Spectrum Software Associates, Chapel Hill, NC). A typical data set consisted of ≥7 spectra, and the spectral information in the 300−850 nm region was used for the analyses. In addition to a dissociation constant, each analysis yielded the spectra of the enzyme, the enzyme−ligand complex, and the free ligand. The spectral data were returned from the program as extinction coefficients at each wavelength, and these data are displayed in various figures. The Factor Analysis of the data for the dithionite titration of $PchF^{C}$ (Figure 1) was carried out using Matlab 5.1 (The Math Works, Inc., Natick, MA). All spectra were corrected for volume changes that occurred on addition of titrants.

An FAD titration of 10 μM apo-PchF at 25 °C in 50 mM Tris-HC1 buffer, pH 7.5, was monitored by the quenching of the flavin fluorescence. The quenching was measured with a Hitachi F-4010 Fluorescence Spectrofluorometer using an excitation wavelength of 446 nm and an emission wavelength of 520 nm.

RESULTS

Properties of E. coli-Produced PchF. In the Materials and Methods section, a procedure is described for the release of proteins from the periplasmic space of *E. coli* using the antibiotic Polymyxin B (*9, 10*). When the periplasmic extract was applied to the Q-Sepharose column, without adding FAD, two PchF peaks were eluted. One peak was due to PchF with tightly, but noncovalently bound FAD, referred to as $PchF^{NC}$, whereas the second peak was PchF without bound FAD. (On denaturating $PchF^{NC}$ with 5% trichloracetic acid, nearly all of the FAD remained in solution after centrifugation.) Therefore, an excess of FAD was added routinely to the extract in order to elute the flavoprotein as a single peak from the Q-Sepharose column. Chromatography of $PchF^{NC}$ on a Ceramic Hydroxyapatite column removed FAD from $PchF^{NC}$. The final step of purification of apo-PchF involved chromatofocusing. Pure apo-PchF was stable on ice for several days at pH 7.5, and in frozen solution at −20 °C for several months. The stability was checked by the ability of the protein to bind FAD, and also by its ability to be converted into holo-PCMH by incubation with PchC and FAD (*1*). PCMH formed in this manner had the same physical properties, steady-state kinetic properties, and stability as the enzyme purified from *P. putida*.

A fluorescence quenching titration of apo-PchF by FAD indicated that the affinity of this protein for the cofactor was sufficiently high that it was not possible to ascertain the dissociation constant. Additionally, the rate of FAD binding to apo-PchF was too fast to measure with the spectrofluorometer.

Dithionite Titrations of $PchF^{C}$ and $PchF^{NC}$. The anaerobic dithionite titration of $PchF^{C}$ was biphasic. The first phase required 1 electron equiv of dithionite to produce a maximum amount of the quasi-stable "red" (anionic) flavin radical (Figure 1) (*13, 14*). For each substoichiometric addition of dithionite in this phase of the titration, end point spectra were reached quickly. For the second phase, approximately 1.5 electron equiv of dithionite were required for full reduction of the bound FAD (Figure 1A, inset), and apparent end point spectra were recorded after 5−15 min. This suggests that

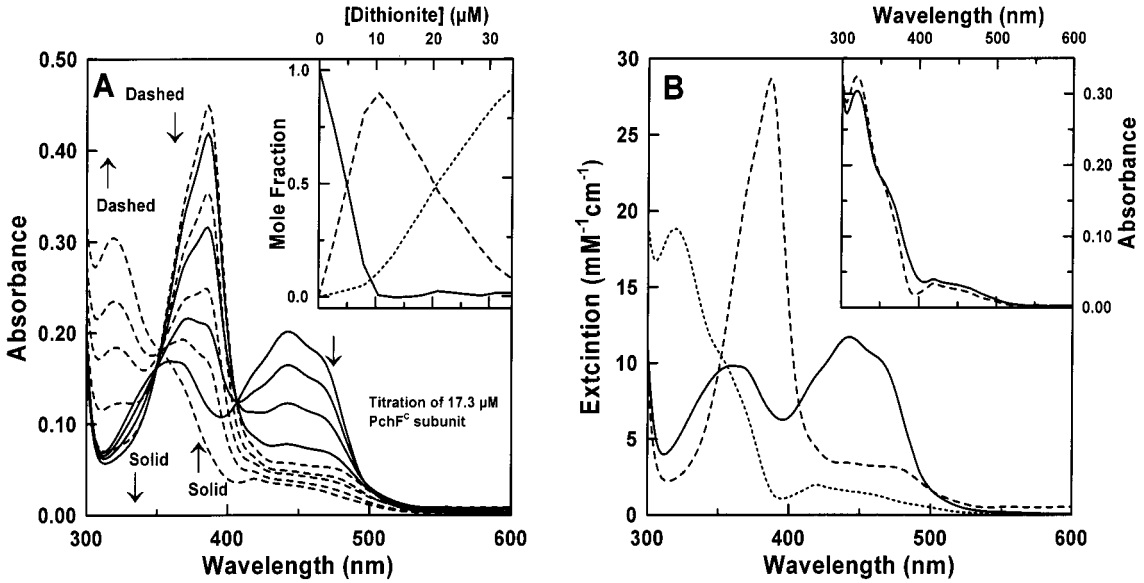

FIGURE 1: Anaerobic dithionite titration of PchF^C. The PchF^C subunit concentration was 17.3 μM in 50 mM potassium phosphate buffer, pH 7.2. (Panel A) This panel displays the apparent end point spectra recorded after the addition of increasing amounts of a standardized dithionite solution. The dithionite concentrations were 0, 2.6, 5.2, and 7.9 μM (solid lines; recorded within a few minutes after the addition of dithionite); and 10.5, 15.7, 20.9, 26.0, and 33.8 μM (dashed lines; recorded 5−15 min after the addition of dithionite). For clarity, the spectra for 13.1, 23.5, 28.6, and 31.2 μM dithionite are omitted. The inset shows a plot of the mole fraction of each species vs the final concentration of dithionite: the oxidized flavoprotein (solid line); the anionic "red" radical (long dashes); the fully reduced flavoprotein (short dashes). These plots were obtained from the Factor Analysis of the spectral data in the main panel A. (Panel B) This panel shows the predicted spectra from the Factor Analysis of the data in panel A. Shown are the spectra of PchF^C with oxidized FAD (solid line), with the bound FAD radical (long dashes), and with fully reduced flavin (short dashes). The inset compares the final spectrum from the titration (solid line, the final spectrum of panel A) and the predicted spectrum of fully reduced PchF^C (dashed line).

the reduction of the protein-bound flavin radical by dithionite was relatively slow, and that the true end points were not attained in this second phase of the titration. The solid line in the inset to Figure 1B is the final recorded spectrum for the titration. The dashed line in the inset represents the true spectrum of fully reduced PchF^C. The spectra for fully reduced enzyme and for the pure flavin radical are shown also in the main panel B of Figure 1.

It is possible that dithionite reacts with fully oxidized protein-bound FAD to produce only the flavin radical. If so, for further reduction to occur, the radical must disproportionate, and the resulting oxidized FAD would immediately react with dithionite, producing more radical. A slow disproportionation and a very slow reaction of radical with dithionite would explain why more than 90% of the maximal amount of radical was formed in the initial stage of the titration (Figures 1A and 1B).

In contrast to the results obtained with PchF^C, the anaerobic dithionite titration of PchF^{NC} proceeded in quite a different manner. In the early part of the titration, there was an isosbestic point at 354 nm. However, as the titration proceeded, the isosbestic point shifted to about 350 nm (Figure 2). Also, a "double-hump" feature is present in the 330−390 nm region of spectra x, y, and z in Figure 2. These attributes suggest that a small amount of red flavin radical may be formed intermediately. Unlike the dithionite titration of PchF^C, the dithionite titration of PchF^{NC} is stoichiometric (Figure 2, inset). Also, the spectra of the fully reduced forms of PchF^C (Figure 1A) and PchF^{NC} exhibit significant differences (Figure 2).

Substrate Titrations of PchF^C and PchF^{NC}. PchF^C was titrated anaerobically with a standardized solution of *p*-cresol (Figure 3). Initially, there was a linear decrease at 443 nm

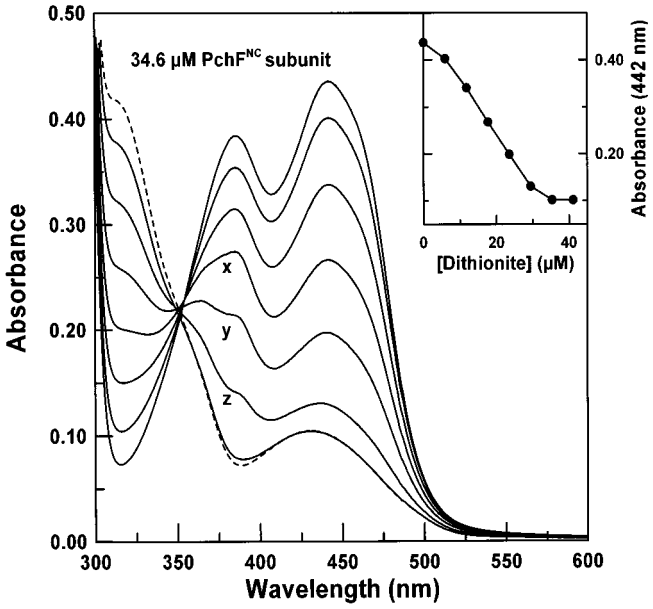

FIGURE 2: Anaerobic dithionite titration of PchF^{NC}. The protein, 34.6 μM (subunit concentration), in 50 mM potassium phosphate buffer, pH 7.3, was titrated anaerobically with a standardized solution of dithionite. The final concentrations of the reductant were 0, 5.9, 11.8, 17.7, 23.6, 29.4, 35.3, and 41.2 μM. The letters x, y, and z mark the regions of three spectra displaying a double-peak feature, which suggests that a trace amount of the anionic flavin radical is formed during the titration. The inset displays a plot of A_{442} vs dithionite concentration.

(Figure 3, inset), and the slope of the linear change provided a $\Delta\epsilon = 11.3$ mM^{-1} cm^{-1}, approximately the value expected for a two-electron reduction by substrate in this portion of the titration. This was unexpected because the product of *p*-cresol oxidation, 4-hydroxybenzyl alcohol, is also a good

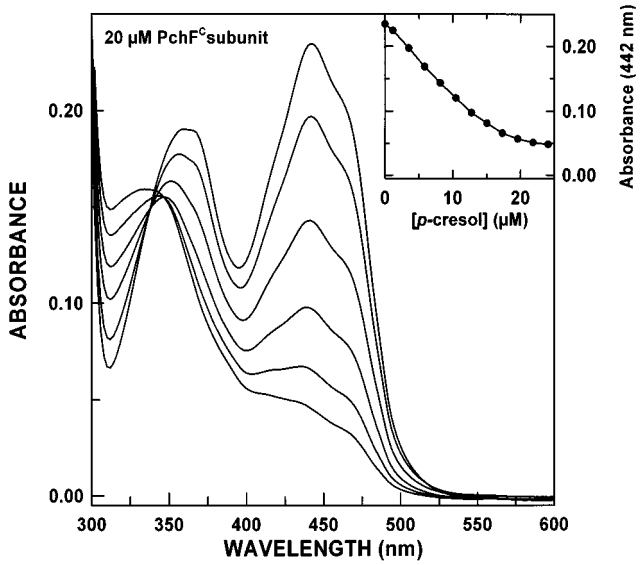

FIGURE 3: Anaerobic *p*-cresol titration of PchF^{C}. The protein (20 μM subunit), in 50 mM potassium phosphate buffer, pH 7.2, was titrated with a standardized solution of *p*-cresol. The final concentrations of *p*-cresol were 0, 3.5, 8.1, 12.8, 17.3, and 24.1 μM. The spectra were recorded 5−10 min after the addition of the reductant. The spectra for 1.2, 5.8, 10.5, 15.0, 19.6, and 21.9 μM *p*-cresol are omitted for clarity. The inset is a plot of A_{442} vs the final concentration of *p*-cresol at each stage of the titration.

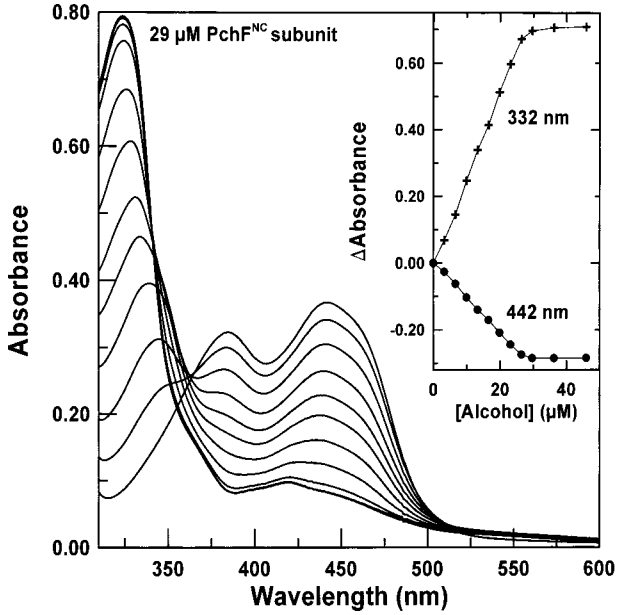

FIGURE 4: Anaerobic titration of PchF^{NC} with 4-hydroxybenzyl alcohol. The protein (29 μM subunit) in 50 mM potassium phosphate buffer, pH 7.2, was titrated with a standardized solution of the alcohol. The final concentrations of titrant were 0, 3.3, 6.6, 10.0, 13.3, 16.6, 19.9, 23.1, 26.4, 29.7, 36.2, and 46.0 μM. Because of the slow reaction, the spectra are those taken 10−90 min after the addition of alcohol. The inset shows the change in absorbances at 442 nm (protein-bound FAD reduction) and 332 nm (formation of 4-hydroxybenzaldehyde).

substrate for PCMH. Thus, we anticipated that 1 mol of *p*-cresol would provide 4 electron equiv for reduction of FAD.

When an anaerobic *p*-cresol titration was terminated after partial reduction of PchF^{C}, an extremely slow, further reduction of the protein-bound FAD and a concomitant increase in absorbance at 330 nm were observed. This suggests very slow release of 4-hydroxybenzyl alcohol from reduced PchF^{C}, followed by free alcohol binding to oxidized PchF^{C} for further FAD reduction. The change at 330 nm reflects the formation of 4-hydroxybenzaldehyde, the product of 4-hydroxybenzyl alcohol oxidation by PchF^{C}.

When an anaerobic solution of PchF^{C} that had been reduced stoichiometrically with *p*-cresol (in the absence of glucose, glucose oxidase, and catalase) was exposed to air, FAD reoxidation and formation of 4-hydroxybenzaldehyde occurred at the same very slow rate. This suggests that the tightly bound alcohol protects FAD from reaction with molecular oxygen. It is only after the alcohol is released that FAD can be rapidly reoxidized by dissolved O_2. The oxidized FAD is very rapidly rereduced by the alcohol, forming 4-hydroxybenzaldehyde. The reduced FAD formed in this step is again reoxidized quickly by dissolved O_2.

As predicted from the experiments described above, when oxidized PchF^{C} was titrated anaerobically with 4-hydroxybenzyl alcohol, a rapid stoichiometric reduction of the bound FAD was observed (1 mol of alcohol/mol of FAD), and a stoichiometric amount of the aldehyde was formed (data not shown).

In contrast to PchF^{C}, it was extremely difficult to reduce anaerobically the FAD bound to PchF^{NC} with *p*-cresol. After 86 h at 4 °C (36 μM enzyme and 4.2 mM *p*-cresol; data not shown), about 40% of the flavin was reduced, and an increase at 330 nm was seen, indicating the formation 4-hydroxybenzaldehyde (see above). Surprisingly, 4-hydroxybenzyl alcohol was considerably more efficient than *p*-cresol in reducing PchF^{NC}. End point spectra were reached in 10−90 min after each substoichiometric addition of the alcohol, and about 1 mol of this material was required to two-electron-reduce 1 mol of protein-bound FAD (Figure 4). Again, there was a large increase in absorbance due to the formation of a stoichiometic amount of 4-hydroxybenzaldehyde (Figure 4, inset). Because of the sluggishness of this reaction, steady-state kinetic assays gave negligible rates using reasonable levels of enzyme.

Spectral Changes Induced by Binding of Substrate and Substrate Analogues. Oxidized PchF^{C} was titrated aerobically with 4-hydroxybenzaldehyde (Figure 5). Factor Analysis of the spectral data provided a $K_D = 0.53$ μM. The analysis also provided spectra and extinction coefficients of the PchF^{C}−ligand species, and the free ligand (Figure 5). The λ_{max} for free 4-hydroxybenzaldehyde is 329 nm ($\epsilon = 10.6$ mM^{-1} cm^{-1}), and the λ_{max} for PchF^{C}−ligand is 342 nm ($\epsilon = 31.6$ mM^{-1} cm^{-1}). At pH 7.2, 4-hydroxybenzaldehyde is about 50% deprotonated (uncharged aldehyde has inconsequential absorbance at 329 nm). Thus, the extinction coefficient of fully deprotonated, free aldehyde is about 21 mM^{-1} cm^{-1}. The large extinction coefficient, relative to free ligand, suggests that 4-hydroxybenzaldehyde is bound as the phenolate (anionic) form, which may be subjected to a polarizing effect from hydrogen bonds, to give a quinone methide species (Figure 6, step III). The partial or complete formation of this species causes the bathochromic shift from 329 nm to about 339−340 nm (corrected from 342 nm for the underlying flavin absorbance). A similar argument has been invoked to explain the bathochromic shifts in λ_{max} following the binding of para-substituted aromatic acyl-CoA thioesters to the medium-chain acyl-CoA dehydrogenase (*15, 16*).

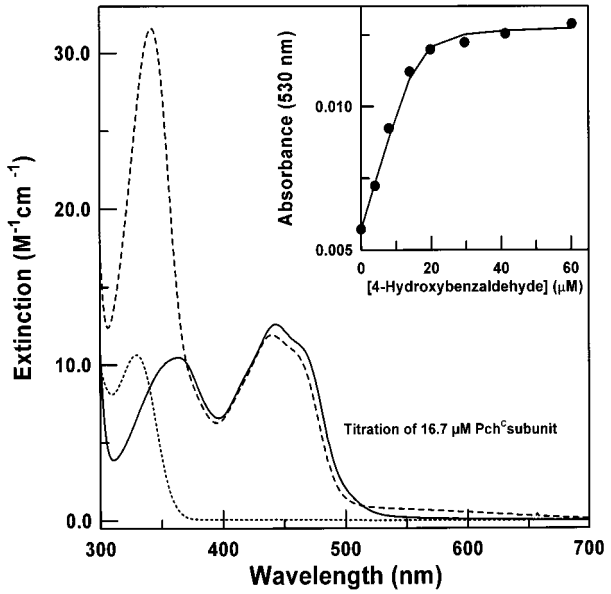

FIGURE 5: Results of an aerobic titration of PchF^C with 4-hydroxybenzaldehyde. This figure displays the spectra obtained from a Factor Analysis of spectra recorded during the titration of this PchF^C (16.7 μM subunit in 50 mM potassium phosphate buffer, pH 7.2) with the aldehyde. The final concentrations of titrant were 0, 4.0, 8.0, 13.9, 19.8, 29.6, 41.2, and 60.3 μM. The solid line is the spectrum for unmodified PchF^C. The line with the long dashes is the spectrum of the PchF^C−aldehyde complex, and the line with the short dashes represents the spectrum of the free aldehyde. These spectra were obtained from a Factor Analysis of the titration data. The inset shows a plot of A_{530} vs the concentration of aldehyde (solid circles, experimental data; the solid line was generated by the Factor Analysis).

Oxidized PchF^{NC} was titrated also with 4-hydroxybenzaldehyde (Figure 7), and the results are similar to those seen for the analogous titration of PchF^C. The Factor Analysis gave the following values: K_D = 0.8 μM; for free 4-hydroxybenzaldehyde, λ_{max} = 330 nm (ϵ = 10.7 mM^{-1} cm^{-1}); for the PchF^C−ligand, λ_{max} = 343 nm (ϵ = 29.6 mM^{-1} cm^{-1}). As is the case for PchF^C, it appears that the anionic form of the aldehyde binds and, at least to some extent, tautomerizes to the quinone methide species shown in Figure 6, step III. The spectra of PchF^C and PchF^{NC} with bound 4-hydroxybenzaldehyde suggested charge-transfer interactions between this aromatic ligand and the isoalloxazine ring of FAD; note the increased absorbance in the 500−700 nm range in Figures 5 and 7.

Because the reduction by *p*-cresol is extremely slow, it was possible to titrate PchF^{NC} aerobically with this substrate (Figure 8). *p*-Cresol bound to PchF^{NC} resulted in a more pronounced charge-transfer peak (Figure 8) than that produced by 4-hydroxybenzaldehyde (Figure 7). The analysis of the data provided a K_D = 233 μM, which is considerably higher than the K_D value of 16 μM determined for *p*-cresol binding to PCMH (*5*).

To investigate the charge-transfer phenomenon further, PchF^C and PchF^{NC} were titrated with the substrate analogue 4-bromophenol (Figures 9 and 10). With this compound, dramatic charge-transfer interactions with the flavins of both forms of PchF are revealed by large absorbances in the 500−900 nm region. The K_D values were found to be 18 μM for PchF^C, and 58 μM for PchF^{NC}. The former value is similar to the K_i value determined for 4-bromophenol in *p*-cresol/PCMH steady-state kinetic assays of PCMH (unpublished observation).

DISCUSSION

The flavoprotein subunit (PchF) of PCMH is the first and only example of a protein that normally binds FAD covalently to be isolated in a stable apo-form, or in a stable form harboring noncovalently bound flavin. Previously, we demonstrated that the FAD covalently bound to PchF only when the PchC cytochrome subunit was present, and in the process of forming the covalent bond, the PchF-bound FAD became two-electron-reduced. Thus, PCMH provides a good system for studying the step-by-step assembly of a mini-electron-transport chain: apo-PchF + FAD → PchF^{NC} + PchC$_{ox}$ → PchF$^C_{red}$/PchC$_{ox}$ → PchF$^C_{rad}$/PchC$_{red}$ → PCMH$_{ox}$ (subscripts "ox", "red", and "rad" indicate oxidized, reduced, and radical forms, respectively). In addition, our studies of this system have provided some insight into the raison d'etre for the covalent linkage (*1*). To address these issues systematically, a comparative study of the basic properties of PchF^C and PchF^{NC} was initiated.

The tight binding of FAD to apo-PchF suggests that there are significant noncovalent interactions between the protein and the flavin. Inspection of the 2.5 Å structure of PCMH indicates that, in addition to the covalent linkage, there are 24 hydrogen bonds between the protein and bound FAD (*17*). For PchF^{NC}, the covalent bond does not seem to be necessary to prevent the undesirable loss of FAD. However, we could

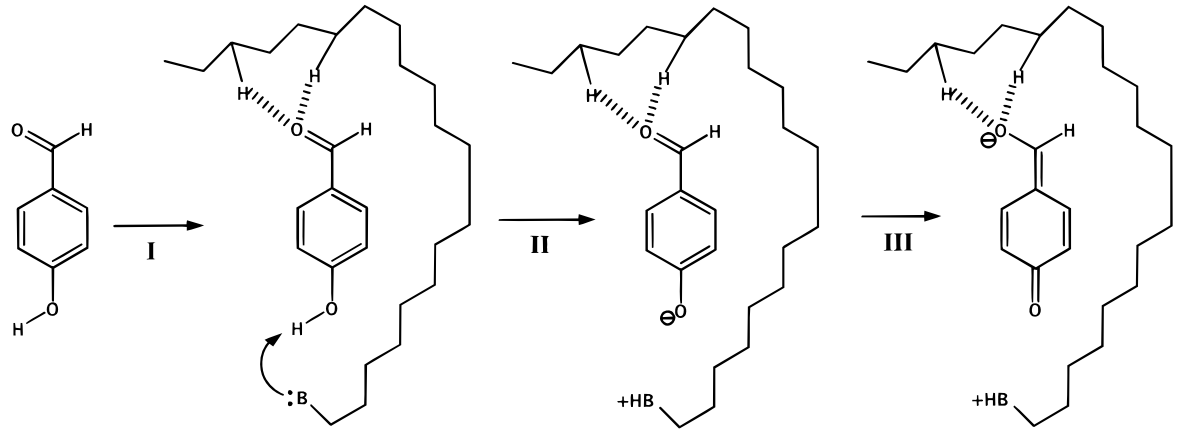

FIGURE 6: Binding of 4-hydroxybenzaldehyde at the active site of PchF^C and PchF^{NC}. By analogy with *p*-cresol binding, it is assumed that the neutral form of the aldehyde binds (step 1). Once bound, 4-hydroxybenzaldehyde is deprotonated (step 2), and then it tautomerizes to a quinone methide species (step 3).

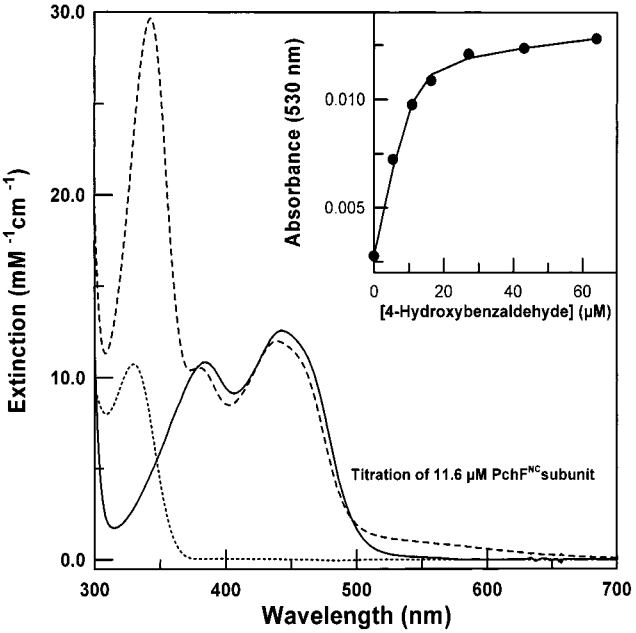

FIGURE 7: Results of an aerobic titration of PchF^{NC} with 4-hydroxybenzaldehyde. The protein (11.6 μM subunit) in 50 mM potassium phosphate buffer, pH 7.2, was titrated with a stock solution of the aldehyde. The final concentrations of the aldehyde were 0, 5.5, 10.9, 16.4, 27.2, 43.1, and 60.1 μM. The solid line represents the spectrum of the unreacted enzyme, the line with the long dashes represents the spectrum of the PchC^{NC}−aldehyde complex, and the curve with the short dashes shows the spectrum of the free aldehyde. The spectra are those obtained from the Factor Analysis of the titration data. The inset shows a plot of A_{530} vs the concentration of 4-hydroxybenzaldehyde. The solid circles are the experimental data, and the solid line is that derived from the Factor Analysis.

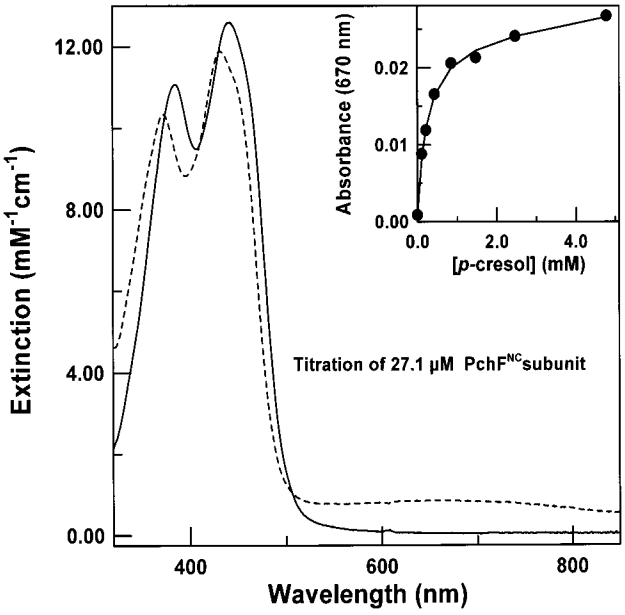

FIGURE 8: Aerobic, nonreductive reaction of PchF^{NC} with *p*-cresol. PchF^{NC} (27.1 μM subunit) in 50 mM potassium phosphate buffer, pH 7.2, was titrated with a stock solution of *p*-cresol over a 15 min period. The initial (solid line) and final (dashed line) spectra are displayed. The final spectrum is that of the oxidized PchF^{NC}/*p*-cresol complex, as determined by the Factor Analysis of the titration data. The concentrations of added *p*-cresol were 0, 0.11, 0.22, 0.43, 0.85, 1.47, 2.47, and 4.78 mM. End points were reached immediately. The inset shows a plot of A_{670} vs the concentration of added *p*-cresol. The solid circles are the experimental points, and the continuous line is derived from the Factor Analysis.

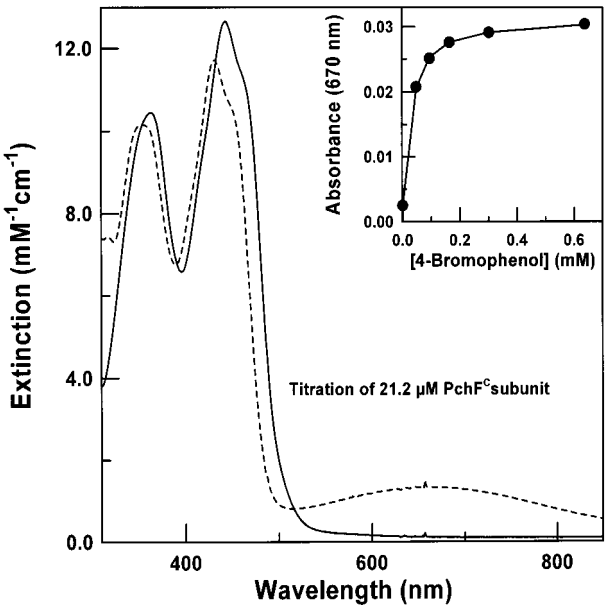

FIGURE 9: Titration of PchF^{C} with 4-bromophenol. The protein (21.2 μM subunit) in 50 mM potassium phosphate buffer, pH 7.2, was titrated with a stock solution of 4-bromophenol: solid line, the spectrum of unreacted enzyme; dashed line, the spectrum of the PchF^{C}/4-bromphenol complex obtained from a Factor Analysis of the titration data. The final concentrations of titrant were 0, 0.046, 0.095, 0.163, 0.301, 0.638, and 1.67 mM. The inset shows a plot of A_{670} vs the concentration of added 4-bromophenol. The solid circles are the experimental points, and the continuous line is derived from the Factor Analysis.

not detect any activity in steady-state assays for PchF^{NC} using *p*-cresol as the substrate. Consequently, covalent binding of FAD to Tyr-384 of PchF must be important for flavin alignment at the active site, and for the disposition of active site amino acyl groups that are required for substrate binding and oxidation. However, these structural features alone must not be optimal for catalysis since PchF^{C} has only 2% of the activity of PCMH, although the K_M values for *p*-cresol are similar for both proteins (*5*, *13*). These observations suggest that PchC binding to PchF^{NC} not only is required for the formation of the covalent bond between PchF and FAD but also contributes to the structural framework required for optimal substrate oxidation.

An altered active site structure is suggested also by the anaerobic *p*-cresol titration of PchF^{C}. Apparently, the product of *p*-cresol oxidation, 4-hydroxybenzyl alcohol, dissociates very slowly from reduced PchF^{C}. If the alcohol were to dissociate rapidly, it would quickly bind to oxidized PchF^{C}, which would become reduced with concomitant formation of 4-hydroxybenzaldehyde. However, this was not observed. Perhaps the tight binding of the alcohol is the result of strong hydrogen bonding interactions between its $-CH_2OH$ group and amino acyl groups at the active site of PchF^{C}. It would seem that the association of PchC with PchF^{C} is required also for efficient product release.

The titrations of PchF^{C} and PchF^{NC} with 4-hydroxybenzaldehyde indicate that a charge-transfer interaction occurs between this compound and the oxidized protein-bound FAD. Data from these titrations indicate also that 4-hydroxybenzaldehyde is bound as the phenolate form in both PchF^{C} and PchF^{NC}. Charge-transfer interactions between bound phenols and FAD were confirmed in a nonreductive titration of

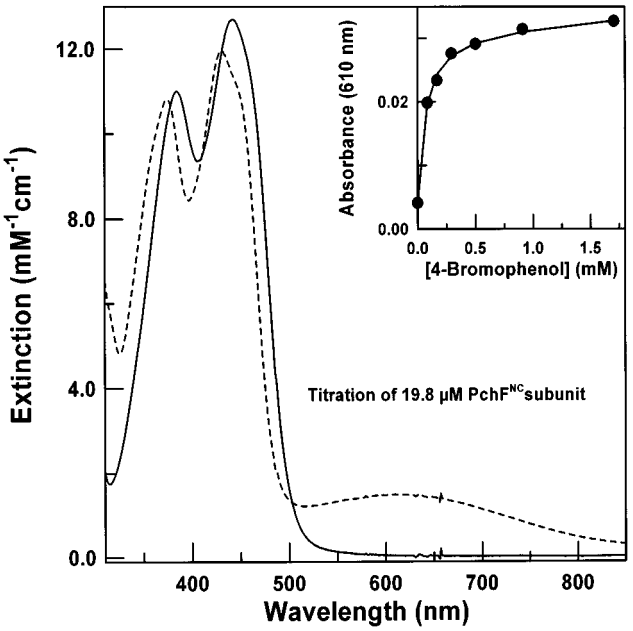

FIGURE 10: Titration of PchF^{NC} with 4-bromophenol. The protein (19.8 μM subunits), in 50 mM potassium phosphate, pH 7.2, buffer, was titrated with a stock solution of 4-bromophenol: solid line, the spectrum of unreacted enzyme; dashed line, the spectrum of the PchF^{NC}/4-bromphenol complex obtained from a Factor Analysis of the titration data. The final concentrations of titrant were 0, 0.084, 0.169, 0.294, 0.502, 1.71, and 3.56 mM. The inset shows a plot of A_{670} vs the concentration of added 4-bromophenol. The solid circles are the experimental points, and the continuous line is that derived from the Factor Analysis.

PchF^{NC} with *p*-cresol, and in titrations of both PchF^{C} and PchF^{NC} with 4-bromophenol. These charge-transfer interactions are reminiscent of those seen on the binding of substituted phenols to Old Yellow Enzyme (*18*, *19*), although the interactions are stronger for this enzyme than for PchF^{C} or PchF^{NC}, as judged by the extinction coefficients of the charge-transfer bands.

A comparison of the 2.5 Å structure of PCMH with the 2.8 Å structure of the PCMH/*p*-cresol complex indicates that the structural changes that occur upon substrate binding are limited to the active site region (*17*). Substrate binding displaces several active site water molecules, and causes the flavin ring to move ~1 Å closer to the heme. The plane of the aromatic moiety of the substrate stacks over the pyrazine/pyrimidine portion of the flavin approximately parallel to the plane of the isoalloxazine ring. A similar disposition of substrate or substrate analogues bound to PchF^{C} and PchF^{NC} would explain the charge-transfer bands observed in the UV− visible spectra.

In order for PCMH to oxidize *p*-cresol, the substrate must have its phenolic proton removed (*17*). Inspection of the structure of the PCMH/*p*-cresol complex indicates that the catalytic base that removes the phenolic proton from *p*-cresol is likely to be either Tyr-95 or Tyr-473. The side-chain hydroxyl groups of both are within hydrogen bonding distance of the substrate hydroxyl group in the PCMH/*p*-cresol complex (*17*). It is assumed that the same base also removes the phenolic proton from 4-hydroxybenzaldehyde bound to PchF^{C} or PchF^{NC} (Figure 6).

It has been suggested that the covalent binding of an aminoacyl group in a protein at the 8-methyl position of FAD prevents the formation of a reactive iminoquinone methide form of the flavin (*3*). The 6-, 8α-, and possibly the 9-positions of the iminoquinone methide would be susceptible to undesirable nucleophilic attack by water or an aminoacyl side group. It is also possible that substitution of the 8-methyl group alters the electronic properties of the flavin in a manner that is beneficial to catalysis, such as providing the flavin with a more positive redox potential (*20*). When free in solution, 8α-aminoacylriboflavin derivatives have $E_{m,7}$ in the range of −150 to −170 mV. These values are 30−50 mV more positive than the $E_{m,7}$ for unmodified free riboflavin (*2*, *21*). It is possible that the different reactivities of PchF^{C} and PchF^{NC} toward substrates, substrate analogues, and dithionite are due solely to differences in the redox potentials of covalently and noncovalently bound FAD. Unfortunately, we have yet to find a reliable way to measure the redox potential of FAD in PchF^{C} or PchF^{NC}.

We have observed that the structures of the flavoprotein subunits of vanillyl alcohol oxidase (VAO) and PCMH are very similar, particularly in the active site/flavin binding regions (*17*). Although VAO is an α_8 oxidase (*22*) and PCMH is an $\alpha_2\beta_2$ dehydrogenase/electron transferase, these enzymes catalyze similar reactions. In PCMH, the tyrosyl residue covalently bound to the flavin appears to be part of the most efficient electron-transfer pathway from reduced FAD to the heme of PchC (*1*, *17*). In VAO, FAD is covalently bound to His-422. However, being an oxidase, VAO does not require electron transfer to another redox group. Molecular oxygen reacts directly with reduced FAD in this protein, so the need for covalent flavin attachment in VAO remains obscure.

In addition to PCMH and VAO, the structures of several other covalent flavoproteins are known. These proteins are the trimethylamine dehydrogenase from *Methylophilus methylotrophus* W3A1 (6-*S*-cysteinyl-FMN) (*23*, *24*), the *E. coli* fumarate reductase membrane−respiratory complex [8α-*N*(3)-histidyl-FAD] (*25*), the flavocytochrome *c* sulfide dehydrogenase (8α-*S*-cysteinyl-FAD) from *Chromatium vinosum* (*26*, *27*), and the monomeric sarcosine oxidase (8α-*S*-cysteinyl-FAD) from *Bacillus* sp. B-0618 (*28*). An important structural feature shared by these enzymes, with the exclusion of the sulfide dehydrogenase, is that all have a guanidino group of an arginine or the ϵ-amino group of a lysine within a few angstroms of the N(1)/C(2)═O part of the flavin ring. For sulfide dehydrogenase, the positive end of a helix dipole substitutes for the positive charge of arginine (*26*, *27*). Along with a nearby lysyl ϵ-amino group, sarcosine oxidase has also the positive end of a helical dipole near this part of the flavin isoalloxazine ring. A positively charged environment near this flavin locus is required for covalent bond formation (*1*, *3*). Additionally, at neutral pH, covalent flavoproteins form anionic (red) flavin radicals, as opposed to neutral (blue) radicals during reductive titrations. A neighboring positive charge provides a stabilizing environment for the anionic radical, which has its negative charge localized at the N(1)/C(2)═O part of the isoalloxazine ring (*29*). The guanidino group of Arg-474 is in close proximity to the N(1)/C(2) locus of FAD in PCMH (*1*, *17*), and is likely to be the case in PchF^{C}, since the anionic radical can be stabilized during the dithionite titration. Little or no radical was observed during the dithionite titration of PchF^{NC}, suggesting that the geometry of flavin binding to PchF^{NC} is altered such that the guanidino group of Arg-474 may be

remote from the N(1)/C(2) locus of the flavin ring.

The spectra of the oxidized and two-electron reduced forms of $PchF^{C}$ and $PchF^{NC}$ also suggest significant environmental differences in the vicinity of the isoalloxazine ring for covalently bound and noncovalently bound FAD (Figures 1B and 2). The partial resolution of the vibrational bands for the long-wavelength peak in the spectrum of oxidized $PchF^{C}$ (Figures 1 and 3) indicates a somewhat hydrophobic environment for the FAD isoalloxazine ring. This fine structure is not seen in the spectrum of oxidized $PchF^{NC}$ (Figure 2).

Obviously, covalent tethering has profound effects on the physical properties and reactivities of FAD in PchF. Efforts are currently in progress to obtain crystals of both $PchF^{C}$ and $PchF^{NC}$ that will be suitable for X-ray crystallographic analysis, to understand at the molecular level the differences in their properties.

REFERENCES

1. Kim, J., Fuller, J. H., Kuusk, V., Cunane, L., Chen, Z.-W., Mathews, F. S., and McIntire, W. S. (1995) *J. Biol. Chem. 270*, 31202−31209.
2. McIntire, W. S., Edmondson, D. E., Hopper, D. J., and Singer, T. P. (1981) *Biochemistry 20*, 3068−3075.
3. Mewies, M., McIntire, W. S., and Scrutton, N. S. (1998) *Protein Sci. 7*, 7−20.
4. Fraaije, M. W., van Berkel, W. J. H., Benen, J. A. E., Visser, J., and Mattevi, A. (1998) *Trends Biochem. Sci. 23*, 206−207.
5. McIntire, W. S., Hopper, D. J., and Singer, T. P. (1987) *Biochemistry 26*, 4107−4117.
6. Kim, J., Fuller, J. H., Cecchini, G., and McIntire, W. S. (1994) *J. Bacteriol. 176*, 6349−6361.
7. Cronin, C. N., Kim, J., Fuller, J. H., Zhang, X., and McIntire, W. S. (1999) *DNA Sequence 10*, 7−17.
8. Cronin, C. N. (1997) *Eur. J. Biochem. 247*, 1029−1037.
9. Fabianek, R. A., Huber-Wunderlich, M., Glockshuber, R., Künzler, P., Hennecke, H., and Thöny-Meyer, L. (1997) *J. Biol. Chem. 272*, 4467−4473.
10. Wiese, A., Münstermann, M., Gutsmann, T., Lindner, B., Kawahara, K., Zähringer, U., and Seydel, U. (1998) *J. Membr. Biol. 162*, 127−138.
11. Edmondson, D. E., and Singer, T. P. (1973) *FEBS Lett. 64*, 255−265.
12. McIntire, W. S. (1983) Ph.D. Thesis, University of California, Berkeley.
13. McIntire, W. S., Hopper, D. J., and Singer, T. P. (1985) *Biochem. J. 228*, 325−335.
14. Massey, V., and Hemmerich, P. (1980) *Biochem. Soc. Trans. 8*, 246−257.
15. Vock, P., Engst, S., Eder, M., and Ghisla, S. (1998) *Biochemistry 37*, 1848−1860.
16. Engst, S., Vock, P., Wang, M., Kim, J. P., and Ghisla, S. (1998) *Biochemistry 37*, 257−267.
17. Cunane, L. M., Chen, Z.-W., Shamala, N., Mathews, F. S., Cronin, C. N., and McIntire, W. S. (1999) *J. Mol. Biol.*, accepted for publication.
18. Abramovitz, A. S., and Massey, V. (1976) *J. Biol. Chem. 251*, 5327−5336.
19. Karplus, P. A., Fox, K. M., and Massey, V. (1995) *FASEB J. 9*, 1518−1526.
20. Meyer, T. E., Bartsch, R. G., Caffrey, M. S., and Cusanovich, M. A. (1991) *Arch. Biochem. Biophys. 287*, 128−134.
21. Edmondson, D. E., and De Francesco, R. (1991) in *Chemistry and Biochemistry of Flavoenzymes* (Muller, F., Ed.) Vol. I, pp 73−103, CRC Press, Boca Raton, FL.
22. Mattevi, A., Fraaije, M. W., Mozzarelli, A., Oliva, L., Coda, A., and van Berkel, W. J. H. (1997) *Structure 5*, 907−920.
23. Bellamy, H. D., Lim, L. W., Mathews, F. S., and Dunham, W. R. (1989) *J. Biol. Chem. 264*, 11887−11892.
24. Lim, L. W., Shamala, N., Mathews, F. S., Steenkamp, D. J., Hamlin, R., and Xuong, N. H. (1986) *J. Biol. Chem. 261*, 15140−15146.
25. Iverson, T. M., Luna-Chavez, C., Cecchini, G., and Rees, D. C. (1999) *Science 284*, 1961−1966.
26. Chen, Z. W., Koh, M., Van Driessche, G., Van Beeumen, J. J., Bartsch, R. G., Meyer, T. E., Cusanovich, M. A., and Mathews, F. S. (1994) *Science* 266, 430−432.
27. Van Driessche, G., Koh, M., Chen, Z. W., Mathews, F. S., Meyer, T. E., Bartsch, R. G., Cusanovich, M. A., and van Beeumen, J. J. (1996) *Protein Sci. 5*, 1753−1764.
28. Trickey, P., Wagner, M. A., Jorns, M. S., and Mathews, F. S. (1999) *Structure 7*, 331−345.
29. Massey, V., and Hemmerich, P. (1980) *Biochem. Soc. Trans. 8*, 246−257.

BI991273D